Quantum Electronics **37** (5) 453 – 464 (2007)

NONLINEAR OPTICAL PHENOMENA

PACS numbers: 42.50 Gy; 42.50.Hz; 42.62.Fi
DOI: 10.1070/QE2007v037n05ABEH013308

Anomalous absorption of light under nonresonance conditions

A.I. Parkhomenko, A.M. Shalagin

***Abstract*. The absorption spectrum of a weak probe field in atomic vapours of rubidium, cesium and samarium in the presence of a strong field is studied theoretically. It is shown that away from resonance with an atomic transition, the probe radiation may have an anomalously high absorption coefficient (several times higher than the resonance value) in an anomalously narrow spectral range. The ultranarrow resonance in the probe-field absorption line wing is not related to any real transitions in the atom. Its position is determined by detuning from resonance frequency and by the strong-field intensity. It is shown that for identical frequencies of the strong and probe waves, the resonance can be recorded by using weak magnetic fields. The effect can be applied in the ultrahigh resolution spectroscopy and for precision measurements of the magnetic field strength.**

Keywords: *probe field, spectroscopy, absorption of light, collisions, coherence*.

1. Introduction

The probe-field spectroscopy of three-level systems involves the investigation of weak (probe) field absorption under conditions when a high-intensity electromagnetic field acts on another (adjoining) transition [1 – 3]. A whole range of effects observed during interaction of radiation with three-level systems (for example, coherent population trapping [4, 5], electromagnetically induced transparency [6], and lasing without inversion [4 – 7]) are manifested most clearly in the three-level Λ-system with two closely spaced lower levels optically coupled with the third, remote upper level. It is this reason that the Λ-system is one of the most actively investigated systems.

The absorption spectrum of a weak probe field by three-level Λ-system atoms was studied in a strong field at the adjacent transition in recent theoretical work [8]. It was assumed that the atoms are located in a buffer gas atmosphere and undergo collisions with its particles. The general case of arbitrary collisional relaxation of the low-frequency coherence at the transition between two lower levels was considered (collisional relaxation could be absent or, on the contrary, could be quite efficient). In the case of copropagating waves and weak collisional relaxation of the low-frequency coherence, an ultranarrow resonance exhibiting a quite unusual behaviour was observed in the probe-field absorption spectrum [8]: the amplitude of this resonance remained unchanged with increasing detuning of the radiation frequency from the resonance frequency being the same even at the far wing of the absorption line as near the line centre. The resonance width decreases rapidly with increasing frequency detuning and may become much smaller than the natural width of the absorption line.

Under certain conditions, a situation may arise when the resonance amplitude at the far wing of the absorption line will even greatly exceed the amplitude of the resonance near the line centre. This contradicts the adopted concept that the cross section of nonresonance radiative processes is always smaller than the cross section of resonance processes. These peculiarities of the probe-field spectrum were discovered in [8] for an idealised three-level Λ-system. The aim of our paper is to prove the existence of anomalous absorption of light for real objects under nonresonance conditions.

A.I. Parkhomenko, A.M. Shalagin Institute of Automation and Electrometry, Siberian Branch, Russian Academy of Sciences, prosp. akad. Koptyuga,1, Novosibirsk, 630090 Russia;
e-mail: par@iae.nsk.su, shalagin@iae.nsk.su

Received 20 June 2006
Kvantovaya Elektronika **37** (5) 453 – 464 (2007)
Translated by Ram Wadhwa

2. Alkali metal atoms

Among the objects promising for observing anomalous absorption of light under nonresonance conditions, we consider first alkali metal atoms. Figure 1 shows the ground state and the first excited level of alkali metals with the nuclear spin $I = 3/2$ (^{7}Li, ^{23}Na, ^{39}K, ^{41}K and ^{87}Rb atoms). The $^2S_{1/2}$ ground state and the $^2P^o_{1/2}$ excited state have hyperfine sublevels with total angular momenta $F_g = 1$, 2 and $F_e = 1$, 2, respectively. Each of the hyperfine levels is degenerate in magnetic quantum numbers $|M| \leqslant F$.

Let us assume that the strong wave $\boldsymbol{E}$ and the weak probe wave $\boldsymbol{E}_\mu$ have mutually orthogonal circular polarisations (right-hand polarisation σ^+ and left-hand polarisation σ^-) and are resonant to the $^2S_{1/2} - {}^2P^o_{1/2}$ transition. Under the action of the strong right-hand polarised field alone, all the atoms will occupy the ground state at the $M = 2$ sublevel of the hyperfine component with $F_g = 2$ (this sublevel is indicated by the letter l in Fig. 1; the quantisation axis z is chosen along the direction of radiation propagation). For the left-hand polarised probe field $\boldsymbol{E}_\mu$, only the $|F_g = 2, M = 2\rangle \rightarrow |F_e = 1, M = 1\rangle$ and $|F_g = 2, M = 2\rangle \rightarrow |F_e = 2, M = 1\rangle$ transitions, which weakly depopulate the l level (the $l \rightarrow m$ and $l \rightarrow k$ transitions in the notation of Fig. 1), should be taken into account. Therefore,

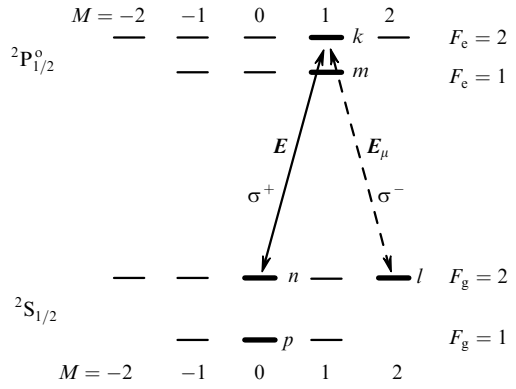

Figure 1. Energy level diagram of alkali metal atoms ^{7}Li, ^{23}Na, ^{39}K, ^{41}K, ^{87}Rb (nuclear spin $I = 3/2$) for the $^2S_{1/2} - {}^2P^o_{1/2}$ transition (D_1 line). The strong ($\boldsymbol{E}$) and probe ($\boldsymbol{E}_\mu$) waves which are resonant to this transition, have mutually orthogonal circular (right-hand σ^+ and left-hand σ^-) polarisations and propagate in the same direction. The quantisation axis is chosen along the direction of radiation propagation.

to determine the probability of absorption of the probe field by the atoms, it is sufficient to consider the interaction of radiation with a subsystem consisting of five sublevels l, m, k, n and p (these sublevels are indicated in bold in Fig. 1).

Similar five-level diagrams can be also selected for other alkali metal atoms (with an arbitrary nuclear spin) also. For example, the levels l, m, k, n and p for ^{133}Cs atoms (nuclear spin $I = 7/2$) correspond to the states $|F_g = 4,\ M = 4\rangle$, $|F_e = 3,\ M = 3\rangle$, $|F_e = 4,\ M = 3\rangle$, $|F_g = 4,\ M = 2\rangle$ and $|F_g = 3,\ M = 2\rangle$, respectively.

The selected system contains four Λ-level diagrams: $n - m - l$, $n - k - l$, $p - m - l$ and $p - k - l$, respectively. This circumstance leads to the assumption that anomalous absorption of light under nonresonance conditions can be observed in alkali metal atoms.

2.1 Initial equations and their solution

Consider the interaction of atoms with a strong monochromatic polarised wave

$$\boldsymbol{E} = \mathrm{Re}E_0\boldsymbol{e}\exp(\mathrm{i}\boldsymbol{k}\boldsymbol{r} - \mathrm{i}\omega t), \tag{1}$$

and a weak monochromatic polarised probe wave

$$\boldsymbol{E}_\mu = \mathrm{Re}E_{0\mu}\boldsymbol{e}_\mu\exp(\mathrm{i}\boldsymbol{k}_\mu\boldsymbol{r} - \mathrm{i}\omega_\mu t), \tag{2}$$

Here, E_0, ω and $E_{0\mu}$ ω_μ, $\boldsymbol{k}_\mu$ are the amplitudes, frequencies and wave vectors of the corresponding waves;

$$\boldsymbol{e} = \sum_{\sigma=0,\pm1} e^{(\sigma)}\boldsymbol{e}_\sigma, \quad \boldsymbol{e}_\mu = \sum_{\sigma=0,\pm1} e^{(\sigma)}_\mu\boldsymbol{e}_\sigma \tag{3}$$

are the unit ($|\boldsymbol{e}| = |\boldsymbol{e}_\mu| = 1$) complex polarisation vectors of the fields and $e^{(\sigma)}$ and $e^{(\sigma)}_\mu$ are their contravariant components in the cyclic basis $\{\boldsymbol{e}_0 = \boldsymbol{e}_z,\ \boldsymbol{e}_{\pm1} = \mp(\boldsymbol{e}_x \pm \boldsymbol{e}_y)/\sqrt{2}\}$. The absorbing particles are located in the mixture with the buffer gas. Collisions between the absorbing particles are neglected and the buffer gas concentration N_b is assumed to be much higher than the concentration N of the absorbing gas. The atoms are described by the five-level diagram (the l, m, k, n and p levels in Fig. 1).

The polarisation of the medium at the probe-field frequency is determined by the elements $\rho_{ml}(\boldsymbol{v})$ and $\rho_{kl}(\boldsymbol{v})$ of the density matrix, where $\boldsymbol{v}$ is the particle velocity. These elements can be found from the system of kinetic equations for the density matrix elements (resonance approximation, steady-state and spatially homogeneous conditions) [1, 2]):

$$\begin{aligned}
&\left[\frac{\Gamma_m}{2} - \mathrm{i}(\Omega_\mu - \boldsymbol{k}_\mu\boldsymbol{v})\right]\rho_{ml}(\boldsymbol{v}) = S(\rho_{ml}(\boldsymbol{v})) + \mathrm{i}G_{\mu ml}[\rho_{ll}(\boldsymbol{v}) \\
&\quad - \rho_{mm}(\boldsymbol{v})] + \mathrm{i}G_{mn}\,\rho_{nl}(\boldsymbol{v}) + \mathrm{i}G_{mp}\,\rho_{pl}(\boldsymbol{v}) - \mathrm{i}G_{\mu kl}\rho_{mk}(\boldsymbol{v}), \\
&\left[\frac{\Gamma_m}{2} - \mathrm{i}(\Omega_\mu - \omega_{km} - \boldsymbol{k}_\mu\boldsymbol{v})\right]\rho_{kl}(\boldsymbol{v}) = S(\rho_{kl}(\boldsymbol{v})) \\
&\quad + \mathrm{i}G_{\mu kl}[\rho_{ll}(\boldsymbol{v}) - \rho_{kk}(\boldsymbol{v})] + \mathrm{i}G_{kn}\,\rho_{nl}(\boldsymbol{v}) \\
&\quad + \mathrm{i}G_{kp}\,\rho_{pl}(\boldsymbol{v}) - \mathrm{i}G_{\mu ml}\rho^*_{mk}(\boldsymbol{v}), \\
&\mathrm{i}(\Omega - \Omega_\mu + \boldsymbol{q}\boldsymbol{v})\rho_{nl}(\boldsymbol{v}) = S(\rho_{nl}(\boldsymbol{v})) + \mathrm{i}G^*_{mn}\,\rho_{ml}(\boldsymbol{v}) \\
&\quad + \mathrm{i}G^*_{kn}\,\rho_{kl}(\boldsymbol{v}) - \mathrm{i}G_{\mu ml}\rho_{nm}(\boldsymbol{v}) - \mathrm{i}G_{\mu kl}\rho_{nk}(\boldsymbol{v}), \\
&\mathrm{i}(\Omega - \Omega_\mu - \omega_{np} + \boldsymbol{q}\boldsymbol{v})\rho_{pl}(\boldsymbol{v}) = S(\rho_{pl}(\boldsymbol{v})) + \mathrm{i}G^*_{mp}\,\rho_{ml}(\boldsymbol{v}) \\
&\quad + \mathrm{i}G^*_{kp}\,\rho_{kl}(\boldsymbol{v}) - \mathrm{i}G_{\mu ml}\rho_{pm}(\boldsymbol{v}) - \mathrm{i}G_{\mu kl}\rho_{pk}(\boldsymbol{v}),
\end{aligned} \tag{4}$$

where

$$\Omega = \omega - \omega_{mn};\ \ \Omega_\mu = \omega_\mu - \omega_{ml};\ \ \boldsymbol{q} \equiv \boldsymbol{k}_\mu - \boldsymbol{k}; \tag{5}$$

$$G_{ij} = \frac{E_0}{2\hbar}\sum_{\sigma=0,\pm1}\langle i|d_\sigma|j\rangle e^{(\sigma)};\ \ G_{\mu ij} = \frac{E_{0\mu}}{2\hbar}\sum_{\sigma=0,\pm1}\langle i|d_\sigma|j\rangle e^{(\sigma)}_\mu;$$

$\rho_{ii}(\boldsymbol{v})$ is the velocity distribution of particles at the ith level ($i = l,\ m,\ k,\ n,\ p$); $S[\rho_{ij}(\boldsymbol{v})]$ are the collision integrals; Γ_m is the rate of spontaneous decay of levels m and k (the spontaneous decay rates are identical for all the magnetic sublevels of the excited state); ω_{ij} is the $i - j$ transition frequency; and $\langle i|d_\sigma|j\rangle$ are the matrix elements of the cyclic component d_σ of the dipole moment for the $|j\rangle = |J_g, I, F_g, M_g\rangle \to |i\rangle = |J_e, I, F_e, M_e\rangle$ transition, which are decribed by the expression [9, 10]

$$\begin{aligned}
&\langle J_e, I, F_e, M_e|d_\sigma|J_g, I, G_g, M_g\rangle = (-1)^{1+I+J_e+F_e+F_g-M_e} \\
&\quad\times\langle J_e||d||J_g\rangle[(2F_e+1)(2F_g+1)]^{1/2} \\
&\quad\times\begin{pmatrix} F_e & 1 & F_g \\ -M_e & \sigma & M_g \end{pmatrix}\begin{Bmatrix} J_e & F_e & I \\ F_g & J_g & 1 \end{Bmatrix};
\end{aligned} \tag{6}$$

$$\begin{pmatrix} a & b & c \\ d & e & f \end{pmatrix} \text{ and } \begin{Bmatrix} a & b & c \\ d & e & f \end{Bmatrix}$$

are the $3j$ and $6j$ symbols [9, 10]; J_e and J_g are the total angular momenta of the electron shell of the atom in the excited and ground state, respectively; M_e and M_g are the projections of the total angular momenta F_e and Fg; and $\langle J_e||d||J_g\rangle$ is the reduced matrix element of the dipole moment.

In the case of mutually orthogonal circular polarisations of strong and probe waves considered here, we should set

$e^{(+1)} = 1$, $e^{(0)} = e^{(-1)} = 0$ (right-hand polarised strong wave, $\sigma = +1$) and $e_\mu^{(-1)} = 1$, $e_\mu^{(0)} = e_\mu^{(+1)} = 0$ (left-hand polarised probe wave, $\sigma = -1$), for the components $e^{(\sigma)}$ and $e_\mu^{(\sigma)}$ of the unit polarisation vectors in (5).

Consider now the case when collisions completely break the phase of the dipole moments induced by the radiation at the $m - l$ and $k - l$ transitions, but the collisional relaxation of low-frequency coherences $\rho_{nl}(\boldsymbol{v})$ and $\rho_{pl}(\boldsymbol{v})$ is arbitrary (can be absent or, on the contrary, can be efficient). For the collision integrals $S[\rho_{ml}(\boldsymbol{v})]$ and $S[\rho_{kl}(\boldsymbol{v})]$ in (4), we use the conventional approximation in this case [1, 3]:

$$S[\rho_{il}(\boldsymbol{v})] = -\nu_1 \rho_{il}(\boldsymbol{v}), \quad i = m, k, \tag{7}$$

where the 'departure' frequency ν_1 is generally a complex quantity (because the potentials of interaction of atoms in the m and k states with buffer particles are almost identical, we can assume that the $m - l$ and $k - l$ transitions have the same impact parameters).

For the collision integrals $S[\rho_{nl}(\boldsymbol{v})]$ and $S[\rho_{pl}(\boldsymbol{v})]$, we will use the strong collisions model [1]:

$$S[\rho_{il}(\boldsymbol{v})] = -\nu \rho_{il}(\boldsymbol{v}) + \tilde{\nu} \rho_{il} W(\boldsymbol{v}), \quad \rho_{il} \equiv \int \rho_{il}(\boldsymbol{v}) \mathrm{d}\boldsymbol{v}, \quad i = n, p,$$
$$W(\boldsymbol{v}) = \frac{\exp\left[(-\boldsymbol{v}/\upsilon_T)^2\right]}{\left(\sqrt{\pi}\upsilon_T\right)^3}, \quad \upsilon_T = \left(\frac{2k_\mathrm{B}T}{M_\mathrm{a}}\right)^{1/2}, \tag{8}$$

where ν and $\tilde{\nu}$ are the 'departure' and 'arrival' frequencies which are complex quantities in the general case (we can assume that the $m - l$ and $k - l$ transitions, and the $n - l$ and $p - l$ transitions also have the same collision parameters); $W(\boldsymbol{v})$ is the Maxwell velocity distribution; k_B is the Boltzmann constant; M_a is the mass of an absorbing particle; and T is the temperature of the medium. The frequency $\tilde{\nu} = 0$ corresponds to the case when collisions lead to a complete relaxation of the coherence $\rho_{il}(\boldsymbol{v})$ (absence of the phase memory during collisions). In the absence of collision relaxation of the coherence $\rho_{il}(\boldsymbol{v})$ (the phase memory is preserved during collisions), the 'departure' and 'arrival' frequencies are equal real quantities [1]:

$$\tilde{\nu} = \nu = \nu_\mathrm{tr}, \tag{9}$$

where ν_tr is the mean transport frequency of elastic collisions of active particles with buffer particles [11]. The quantity ν_tr is related to the diffusion coefficient D of particles interacting with the radiation by the expression $D = \upsilon_T^2/(2\nu_\mathrm{tr})$ [12], where υ_T is the most probable velocity of the absorbing particles.

Because the probe field is weak, we can assume that the matrix elements $\rho_{ll}(\boldsymbol{v})$ and $\rho_{ij}(\boldsymbol{v})$ (where $i, j \neq l$) in Eqns (4) are known and determined only by the action of the strong field. We will assume below that there are no collision $n \leftrightarrow l$ and $p \leftrightarrow l$ transitions between the n, p and l levels. In this case, all the atoms will be transferred to the l level under the action of the strong field only. Therefore, it can be assumed in (4) that

$$\rho_{ll}(\boldsymbol{v}) = NW(\boldsymbol{v}), \ \rho_{ij}(\boldsymbol{v}) = 0, \ ij = mm, kk, nm, pm, mk, nk, pk. \tag{10}$$

Taking (7), (8) and (10) into account, we obtain from the system of equations (4)

$$\lambda_1(\boldsymbol{v})\rho_{ml}(\boldsymbol{v}) = \mathrm{i}G_{\mu ml}NW(\boldsymbol{v}) + \mathrm{i}G_{mn}\rho_{nl}(\boldsymbol{v}) + \mathrm{i}G_{mp}\rho_{pl}(\boldsymbol{v}),$$
$$\lambda_2(\boldsymbol{v})\rho_{kl}(\boldsymbol{v}) = \mathrm{i}G_{\mu kl}NW(\boldsymbol{v}) + \mathrm{i}G_{kn}\rho_{nl}(\boldsymbol{v}) + \mathrm{i}G_{kp}\rho_{pl}(\boldsymbol{v}),$$
$$\lambda_3(\boldsymbol{v})\rho_{nl}(\boldsymbol{v}) = \tilde{\nu}\rho_{nl}W(\boldsymbol{v}) + \mathrm{i}G^*_{mn}\rho_{ml}(\boldsymbol{v}) + \mathrm{i}G^*_{kn}\rho_{kl}(\boldsymbol{v}), \tag{11}$$
$$\lambda_4(\boldsymbol{v})\rho_{pl}(\boldsymbol{v}) = \tilde{\nu}\rho_{pl}W(\boldsymbol{v}) + \mathrm{i}G^*_{mp}\rho_{ml}(\boldsymbol{v}) + \mathrm{i}G^*_{kp}\rho_{kl}(\boldsymbol{v}),$$

where

$$\lambda_1(\boldsymbol{v}) = \frac{\Gamma_m}{2} + \nu_1 - \mathrm{i}(\Omega_\mu - \boldsymbol{k}_\mu\boldsymbol{v}); \quad \lambda_2(\boldsymbol{v}) = \lambda_1(\boldsymbol{v}) + \mathrm{i}\omega_{km};$$
$$\lambda_3(\boldsymbol{v}) = \nu - \mathrm{i}(\Omega_\mu - \Omega - \boldsymbol{q}\boldsymbol{v}); \quad \lambda_4(\boldsymbol{v}) = \lambda_3(\boldsymbol{v}) - \mathrm{i}\omega_{np}. \tag{12}$$

According to the general rules, the probability P_μ of absorption of the probe field at a frequency ω_μ (number of events of absorption of radiation per unit time per absorbing atom) is determined by the expression

$$P_\mu \equiv -\frac{2}{N}\,\mathrm{Re}(\mathrm{i}G^*_{\mu ml}\rho_{ml} + \mathrm{i}G^*_{\mu kl}\rho_{kl}), \tag{13}$$
$$\rho_{il} \equiv \int \rho_{il}(\boldsymbol{v})\mathrm{d}\boldsymbol{v}, \quad i = m, k.$$

Thus, in accordance with the problem formulated here, we must find the quantities ρ_{ml} and ρ_{kl} from the system of equations (11).

According to [8], the narrow resonances in the probe-field absorption wing should appear in the vicinity of the detunings of the probe-field frequency $\Omega_\mu \approx \Omega$ and $\Omega_\mu \approx \Omega - \omega_{np}$. In these detuning regions, the calculation of the probability P_μ of the probe field absorption is considerably simplified because we can assume that $\rho_{pl}(\boldsymbol{v}) = 0$ in the system of equations (11) if P_μ is calculated in the vicinity of $\Omega_\mu \approx \Omega$, or $\rho_{nl}(\boldsymbol{v}) = 0$ if P_μ is calculated in the vicinity of $\Omega_\mu \approx \Omega - \omega_{np}$. Indeed, by integrating the last two equations in (11) with respect to velocities for $\boldsymbol{q} = 0$ and taking into account that $G_{mn} \sim G_{mp} \sim G_{kn} \sim G_{kp}$, we obtain the approximate relation between the matrix elements ρ_{pl} and ρ_{nl}:

$$\frac{\rho_{pl}}{\rho_{nl}} \sim \frac{\nu - \tilde{\nu} - \mathrm{i}(\Omega_\mu - \Omega)}{\nu - \tilde{\nu} - \mathrm{i}(\Omega_\mu - \Omega + \omega_{np})}. \tag{14}$$

If $\boldsymbol{q} \neq 0$, we should supplement the numerator and denominator on the right-hand side of (14) by a term of the order of $\mathrm{i}q\upsilon_T$. Let us assume that the condition:

$$|\nu - \tilde{\nu}|, \quad q\upsilon_T \ll \omega_{np} \tag{15}$$

is satisfied. Then, it follows from (14) that the relation $|\rho_{pl}| \ll |\rho_{nl}|$ is satisfied near the detuning of the probe field frequency $\Omega_\mu \approx \Omega$ (for $|\Omega_\mu - \Omega| \ll \omega_{np}$), and, hence, the matrix element $\rho_{pl}(\boldsymbol{v})$ in the system of equations can be neglected in the description of the corresponding resonance (i.e., the p level can be neglected). Near the detuning $\Omega_\mu \approx \Omega - \omega_{np}$ (for $|\Omega_\mu - \Omega| \ll \omega_{np}$), the inverse relation $|\rho_{nl}| \ll |\rho_{pl}|$ is satisfied, and hence the matrix element $\rho_{nl}(\boldsymbol{v})$ can be neglected in the system of equations (11) (the n level can be neglected).

By neglecting the matrix element $\rho_{pl}(\boldsymbol{v})$ in the system of equations (11) (i.e., by neglecting the p level), we obtain the expression:

$$P_\mu = 2\mathrm{Re}\Big\{|G_{\mu ml}|^2 I_2 + |G_{\mu kl}|^2 I_3 + \Big[|G_{\mu ml}|^2|G_{kn}|^2 + |G_{\mu kl}|^2|G_{mn}|^2 - 2\mathrm{Re}(G_{mn}G_{kn}^* G_{\mu ml}^* G_{\mu kl})\Big] K - \frac{\tilde{\nu}}{1-\tilde{\nu}I_1} \times \Big[|G_{mn}|^2|G_{\mu ml}|^2 J_2^2 + |G_{kn}|^2|G_{\mu kl}|^2 J_1^2 + 2J_1J_2\mathrm{Re}(G_{mn}G_{kn}^* G_{\mu ml}^* G_{\mu kl})\Big]\Big\} \quad (16)$$

for the probe-field absorption probability, where

$$I_1 = \int \frac{\lambda_1(\boldsymbol{v})\lambda_2(\boldsymbol{v})W(\boldsymbol{v})}{D(\boldsymbol{v})}\,\mathrm{d}\boldsymbol{v}; \quad I_2 = \int \frac{\lambda_2(\boldsymbol{v})\lambda_3(\boldsymbol{v})W(\boldsymbol{v})}{D(\boldsymbol{v})}\,\mathrm{d}\boldsymbol{v};$$

$$I_3 = \int \frac{\lambda_1(\boldsymbol{v})\lambda_3(\boldsymbol{v})W(\boldsymbol{v})}{D(\boldsymbol{v})}\,\mathrm{d}\boldsymbol{v}; \quad K = \int \frac{W(\boldsymbol{v})}{D(\boldsymbol{v})}\,\mathrm{d}\boldsymbol{v}; \quad (17)$$

$$J_{1,2} = \int \frac{\lambda_{1,2}(\boldsymbol{v})W(\boldsymbol{v})}{D(\boldsymbol{v})}\,\mathrm{d}\boldsymbol{v};$$

$$D(\boldsymbol{v}) = \lambda_1(\boldsymbol{v})\lambda_2(\boldsymbol{v})\lambda_3(\boldsymbol{v}) + |G_{mn}|^2\lambda_2(\boldsymbol{v}) + |G_{kn}|^2\lambda_1(\boldsymbol{v}).$$

Expression (16) describes resonance in the probe field spectrum in the vicinity of $\Omega_\mu \approx \Omega$ (near the probe field frequency $\omega_\mu \approx \omega$). In the absence of one of the excited levels (k or m), expression (16) coincides, as expected, with the expression obtained in [8] for the probability of absorption of a weak probe field by three-level Λ-system atoms.

The resonance in the probe field spectrum in the vicinity of $\Omega_\mu \approx \Omega - \omega_{np}$ (near the probe-field frequency $\omega_\mu \approx \omega - \omega_{np}$) is described by expressions (16), (17) by using the replacements:

$$G_{mn} \to G_{mp}, \quad G_{kn} \to G_{kp}, \quad \lambda_3(\boldsymbol{v}) \to \lambda_4(\boldsymbol{v}). \quad (18)$$

The values of G_{ij} and $G_{\mu ij}$ in (16) for particular objects can be readily calculated from (5) and (6). For alkali metal atoms with the nuclear spin $I = 3/2$ (^{7}Li, ^{23}Na, ^{39}K, ^{41}K and ^{87}Rb atoms), $I = 5/2$ (^{85}Rb atoms) and $I = 7/2$ (^{133}Cs atoms), expression (16) takes the form

$$P_\mu = 2|G_\mu|^2\mathrm{Re}\left[I_2 + \frac{a_1}{3}\,I_3 + \frac{16a_2}{3}\,|G|^2K - \frac{\tilde{\nu}|G|^2(J_1-J_2)^2}{1-\tilde{\nu}I_1}\right], \quad (19)$$

where

$$|G|^2 = \frac{a_3|\langle J_\mathrm{e}||d||J_\mathrm{g}\rangle|^2E_0^2}{96\hbar^2}; \quad |G_\mu|^2 = \frac{a_4|\langle J_\mathrm{e}||d||J_\mathrm{g}\rangle|^2E_{0\mu}^2}{16\hbar^2}; \quad (20)$$

and the integrals I_{1-3}, $J_{1,2}$, and K are described by expressions (17) for

$$D(\boldsymbol{v}) = \lambda_1(\boldsymbol{v})\lambda_2(\boldsymbol{v})\lambda_3(\boldsymbol{v}) + |G|^2[\lambda_2(\boldsymbol{v}) + 3a_5\lambda_1(\boldsymbol{v})]. \quad (21)$$

Here, a_{1-5} are numerical coefficients. For the ^{7}Li, ^{23}Na, ^{39}K, ^{41}K and ^{87}Rb atoms, the coefficients $a_{1-5} = 1$. For the ^{85}Rb atoms, $a_1 = 3/5$, $a_2 = 27/20$, $a_3 = 4/9$, $a_4 = 10/9$, $a_5 = 5/3$. Finally, for ^{133}Cs atoms, $a_1 = 3/7$, $a_2 = 12/7$, $a_3 = 1/4$, $a_4 = 7/6$, $a_5 = 7/3$.

Taking into account that the reduced matrix element $\langle J_\mathrm{e}||d||J_\mathrm{g}\rangle$ is related to the spontaneous decay rate Γ_m of the excited $^2\mathrm{P}^\mathrm{o}_{1/2}$ state by the expression [10]

$$\Gamma_m = \frac{4\omega_{\mathrm{eg}}^3}{3\hbar c^3}\,\frac{|\langle J_\mathrm{e}||d||J_\mathrm{g}\rangle|^2}{2J_\mathrm{e}+1} \quad (22)$$

where ω_{eg} is the transition frequency, it is convenient to express $|G|^2$ in (20) in terms of the constant Γ_m, the radiation intensity I and the transition wavelength λ:

$$|G|^2 = \frac{a_3\lambda^3\Gamma_m I}{64\pi^2\hbar c}, \quad I = \frac{cE_0^2}{8\pi}. \quad (23)$$

Expression (19) describes a resonance in the probe field spectrum near the frequency $\omega_\mu \approx \omega$ under condition (15), which is always satisfied for copropagating waves at moderate pressures of the buffer gas. The same expression also describes resonance near the probe-field frequency $\omega_\mu \approx \omega - \omega_{np}$ if we make the substitution $\Omega \to \Omega - \omega_{mp}$ in it, i.e., if Ω in (19) is the detuning of the strong-radiation frequency relative to the $m-p$ transition frequency. In this case, the coefficients a_{1-5} in (19)–(21) remain unchanged for all atoms except ^{85}Rb and ^{133}Cs, for which only the coefficient a_3 changes and should be set equal to 8/9 for ^{85}Rb and 3/4 for ^{133}Cs.

2.2 Spectral analysis of the probe field

Figure 2 shows the dependence of the absorption probability P_μ of the probe field of the frequency detuning Ω_μ for the ^{87}Rb atoms ($\lambda = 7947.6$ Å, $\Gamma_m = 0.34 \times 10^8$ s^{-1}, $\omega_{np} = 4.29 \times 10^{10}$ s^{-1}, $\omega_{km} = 5.1 \times 10^9$ s^{-1} [13]), ^{85}Rb atoms ($\omega_{np} = 1.91 \times 10^{10}$ s^{-1}, $\omega_{km} = 2.28 \times 10^9$ s^{-1} [13]), and ^{133}Cs atoms ($\lambda = 8943.5$ Å, $\Gamma_m = 0.33 \times 10^8$ s^{-1}, $\omega_{np} = 5.78 \times 10^{10}$ s^{-1}, $\omega_{km} = 7.34 \times 10^9$ s^{-1} [13]) for copropagating strong and probe waves in the case of a large detuning of the strong field frequency Ω (compared to the Doppler linewidth kv_T). It was assumed that the phase memory is completely preserved during collisions at transitions between the magnetic sublevels of the ground-state hyperfine structure ($\tilde{\nu} = \nu$). The absorption probability P_μ in Figs 2–6 is normalised to the absorption probability P_0 of probe radiation when its frequency is tuned to the centre of the $m-l$ transition line in the low-intensity limit of the strong field. According to (19), we have

$$P_0 = 2|G_\mu|^2\mathrm{Re}\int\left[\frac{1}{\lambda_1(\boldsymbol{v})} + \frac{a_1}{3\lambda_2(\boldsymbol{v})}\right]W(\boldsymbol{v})\mathrm{d}(\boldsymbol{v}), \quad (24)$$

where $\lambda_{1,2}(\boldsymbol{v})$ are described by expressions (12) under the condition $\Omega_\mu - \mathrm{Im}\,v_1 = 0$ determining the centre of the $m-l$ transition line taking into account the collisional shift. In the case of a noticeable separation of the absorption lines at the $m-l$ and $k-l$ transitions (for $\omega_{km} \gtrsim 2k_\mu v_T$) and the Doppler broadening [for $\Gamma \ll k_\mu v_T$, where Γ is the homogeneous half-width of the absorption line, see expression (29) below], it follows from (24) that

$$P_0 = \frac{2\sqrt{\pi}|G_\mu|^2}{k_\mu v_T}. \quad (25)$$

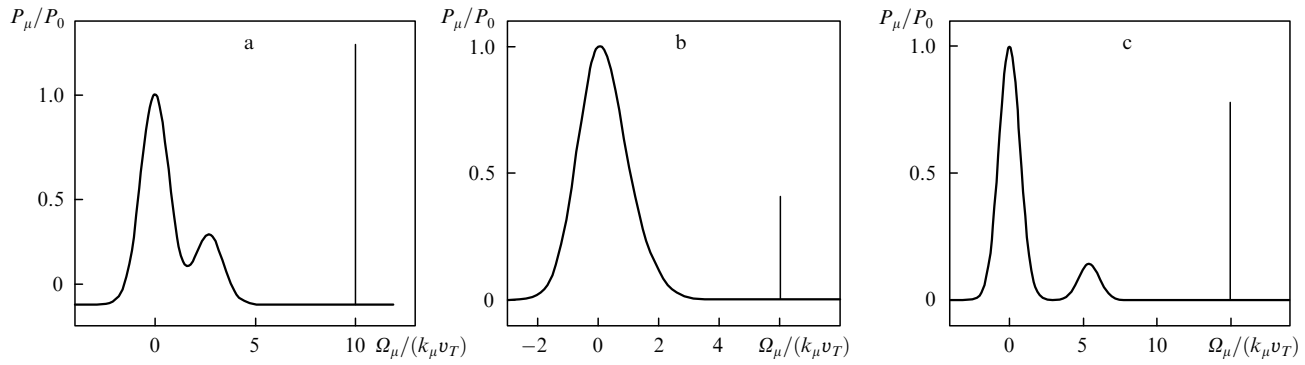

Figure 2. Dependence of the absorption probability P_μ for the probe field on the frequency detuning Ω_μ for (a) ^{87}Rb, (b) ^{85}Rb and (c) ^{133}Cs atoms in the case of copropagating strong and probe waves ($\boldsymbol{q} = 0$) and in the absence of collisional relaxation of the coherence at transitions between the magnetic sublevels of the ground-state hyperfine structure ($\tilde{\nu} = \nu$) at $T = 300$ K, $I = 10^{-3}$ W cm^{-2}, $\nu_1 = \nu$, $\nu/(kv_T) = 3 \times 10^{-4}$, $\Omega/(kv_T) = 10$ (a), 6 (b) and 15 (c). The strong wave and the probe wave have mutually orthogonal (right- and left-hand) circular polarisations. The ultranarrow resonance with a large amplitude appears in the vicinity of $\Omega_\mu \approx \Omega$.

One can see from Fig. 2 that the probe field spectrum consists of two broad resonances (with the Doppler width kv_T) located in the vicinity of $\Omega_\mu = 0$ and $\Omega_\mu = \omega_{km}$, and the ultranarrow resonance with a large amplitude located at the far wing of the absorption line (in the vicinity of $\Omega_\mu \approx \Omega \gg kv_T$). The origin of the broad resonances can be explained trivially: they are caused by absorption of the probe radiation at the $m - l$ and $k - l$ transitions. The ultranarrow resonance at the far wing of the absorption line is not related to any real transitions in the atom. Its position is determined by the frequency detuning and the strong-field intensity. Analysis shows that for $|\Omega|$, $|\Omega - \omega_{km}| > kv_T$ and a moderate radiation intensity for which

$$|G|^2 \ll |\Omega|\omega_{km}, |\Omega - \omega_{km}|\omega_{km}, |\Omega(\Omega - \omega_{km})|, \tag{26}$$

the ultranarrow resonance is located in the vicinity of

$$\Omega_\mu = \Omega + \frac{|G|^2}{\Omega} + \frac{3a_5|G|^2}{\Omega - \omega_{km}}. \tag{27}$$

The first term in the right-hand side of (27) is the main term, while the next two terms, which are proportional to the radiation intensity represent small corrections.

The half-width Γ_w of the resonance in the case of copropagating waves (for $\boldsymbol{q} = 0$) and for

$$|\Omega|, |\Omega - \omega_{km}| \gtrsim 3kv_T, \quad \nu' \gg \frac{k_\mu v_T|G|^2}{\Omega^2}, \frac{k_\mu v_T|G|^2}{(\Omega - \omega_{km})^2} \tag{28}$$

is described by the expression

$$\Gamma_w = \Gamma_1 + \gamma, \tag{29}$$

where

$$\Gamma_1 = (\nu - \tilde{\nu})'; \quad \gamma = \left[\frac{|G|^2}{\Omega^2} + \frac{3a_5|G|^2}{(\Omega - \omega_{km})^2}\right]\Gamma; \quad \Gamma = \frac{\Gamma_m}{2} + \nu_1'. \tag{30}$$

Hereafter, the primed quantities in the text represent real parts of complex numbers. The quantity Γ is the homogeneous half-width of the absorption line at the $m - l$ and $k - l$ transitions, which is determined by the spontaneous decay of the excited state and collisions between particles. For a moderate radiation intensity [see (26)], the parameter γ is always small: $\gamma \ll \Gamma$. The quantity Γ_1 is always small compared to Γ for low buffer gas pressures, and $\Gamma_1 = 0$ at any pressures if the phase memory is preserved during collisions between the magnetic sublevels of the ground-state hyperfine structure. Thus, the width of the resonance may be much smaller than the natural absorption linewidth. For example, for parameters $I = 10^{-3}$ W cm^{-2} and $\nu/(kv_T) = 3 \times 10^{-4}$ (see Fig. 2), the resonance linewidth $2\Gamma_w \sim 1$ Hz, while for parameters $I = 1$ W cm^{-2} and $\nu/(kv_T) = 9 \times 10^{-3}$ [see Fig. 3, curve (*1*)], its value is ~ 3 kHz.

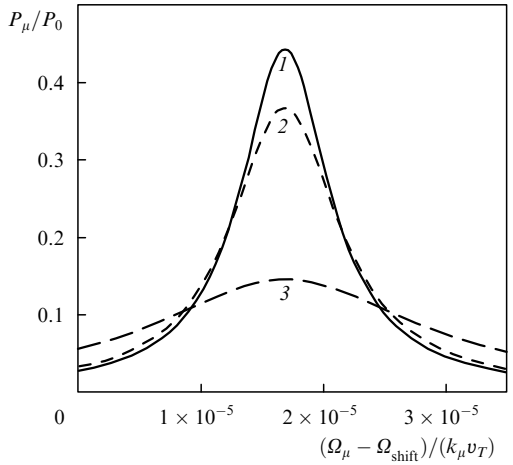

Figure 3. Sensitivity of the dependence $P_\mu(\Omega_\mu)$ in the vicinity of $\Omega_\mu \approx \Omega$ to the degree of phase memory conservation during collisions for ^{87}Rb atoms, $T = 300$ K, $I = 1$ W cm^{-2}, $\Omega/(kv_T) = 10$, $\nu_1 = \nu$, $\nu/(kv_T) = 9 \times 10^{-3}$, $\tilde{\nu} = \nu$ (*1*), $\tilde{\nu}'/\nu' = 0.9999$ (*2*) and 0.999 (*3*); $\Omega_{\text{shift}}/(k_\mu v_T) = 10.00121$.

Collisions play an extremely important role in the resonance formation in the absorption line wing. In the absence of collisions, the resonance amplitude is always small: the relative amplitude $P_\mu^{\max}/P_0$ does not exceed a few percent (here $P_\mu^{\max}$ is the maximum value of P_μ in the vicinity of $\Omega_\mu \approx \Omega$). Collisions which preserve the phase memory at transitions between magnetic sublevels of the ground-state hyperfine structure ($\tilde{\nu} = \nu$) may increase the resonance amplitude by a factor of $k_\mu v_T/(\sqrt{\pi}\Gamma) \gg 1$. For example, for parameters of ^{87}Rb atoms corresponding to

Fig. 2a, the relative resonance amplitude $P_\mu^{\max}/P_0 \approx 1.25$. In the absence of collisions (for $v = 0$ and for unchanged values of the remaining parameters T, I, Ω), the resonance amplitude is smaller by a factor of 60: $P_\mu^{\max}/P_0 \approx 0.02$.

Collisions start affecting the amplitude and width of the resonance at frequencies

$$v' \gtrsim \frac{k_\mu v_T |G|^2}{\Omega^2}, \frac{k_\mu v_T |G|^2}{(\Omega - \omega_{km})^2}. \quad (31)$$

In the case of the Doppler broadening of the absorption line ($k_\mu v_T \gg \Gamma$), which we consider here, expression (31) means that $v' \gg \gamma$. For fixed values of the intensity and detuning of the strong-field frequency (for a fixed value of γ), the amplitude of the resonance is inversely proportional to its width:

$$P_\mu^{\max} \propto \Gamma_w^{-1} = [(v - \tilde{v})' + \gamma]^{-1}. \quad (32)$$

This means that for

$$1 - \frac{\tilde{v}'}{v'} \lesssim \frac{\gamma}{v'} \quad (33)$$

the resonance amplitude is close to its maximum value, which is achieved when the phase memory is completely preserved (for $\tilde{v} = v = v_{tr}$).

For alkali metal atoms in an atmosphere of inert buffer gases, the cross sections for collision transitions between magnetic sublevels of the ground-state hyperfine structure are 6–10 orders of magnitude smaller than the gas-kinetic cross sections [14]. Therefore, we can expect for these objects a high degree of conservation of the phase memory during collisions, such that $1 - \tilde{v}'/v' \lesssim 10^{-6}$. For such an extent of the phase-memory conservation, the resonance amplitude is almost always close to its maximum value, which is achieved for a complete conservation of the phase memory.

Figure 3 shows the sensitivity of the resonance amplitude to the degree of phase memory conservation. The resonance amplitude is close to its maximum value for $\tilde{v}'/v' = 0.9999$ [see curves (*1*) and (*2*) in Fig. 3].

The resonance amplitude in the line wing depends nonmonotonically on the collision frequency. Figure 4 shows the dependence of the resonance amplitude on the collision frequency in the case of phase memory conservation ($\tilde{v} = v$). The resonance amplitude increases at first with v and achieves its maximum value for a certain value of the collision frequency [$v/(kv_T) = 9 \times 10^{-3}$], after which it starts decreasing with increasing v. The value of v (and hence of the buffer gas pressure) for which the maximum of v is achieved depends on the radiation intensity and is the smaller, the lower the intensity. For example, the resonance amplitude for $I = 10^{-3}$ W cm^{-2} achieves its maximum for $v/(kv_T) = 3 \times 10^{-4}$ (these are the starting parameters for Fig. 2), while for $I = 1$ W cm^{-2} the maximum is achieved for $v/(kv_T) = 9 \times 10^{-3}$ (see Fig. 4).

Figure 5 shows the dependence of the relative resonance amplitude $P_\mu^{\max}/P_0$ on the detuning Ω of the strong field frequency for two values of its intensity I (10^{-3} and 1 W cm^{-2}). For each value of I, the collision frequency is chosen in such a way that the resonance amplitude has its maximum. One can see from Fig. 5 that the resonance amplitude decreases with increasing the strong-field intensity. This dependence is quite weak (as the intensity is

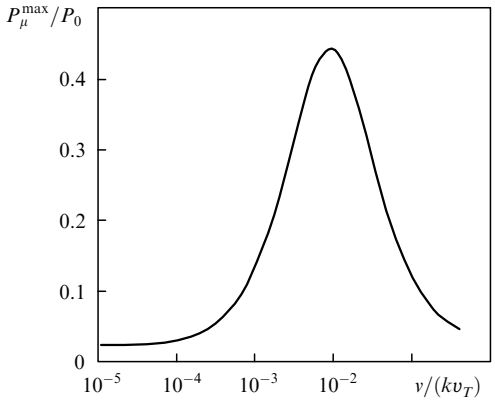

Figure 4. Dependence of the resonance amplitude for ^{87}Rb atoms at the wing of the resonance curve on the collision frequency in the case of phase memory conservation during collisions at transitions between the magnetic sublevels of the ground-state hyperfine structure ($\tilde{v} = v = v_{tr}$), $T = 300$ K, $I = 1$ W cm^{-2}, $\Omega/(kv_T) = 10$, $v_1 = v$.

increased by three orders of magnitude, the resonance amplitude decreases only by several times). As the frequency detuning increases, the resonance amplitude first increases

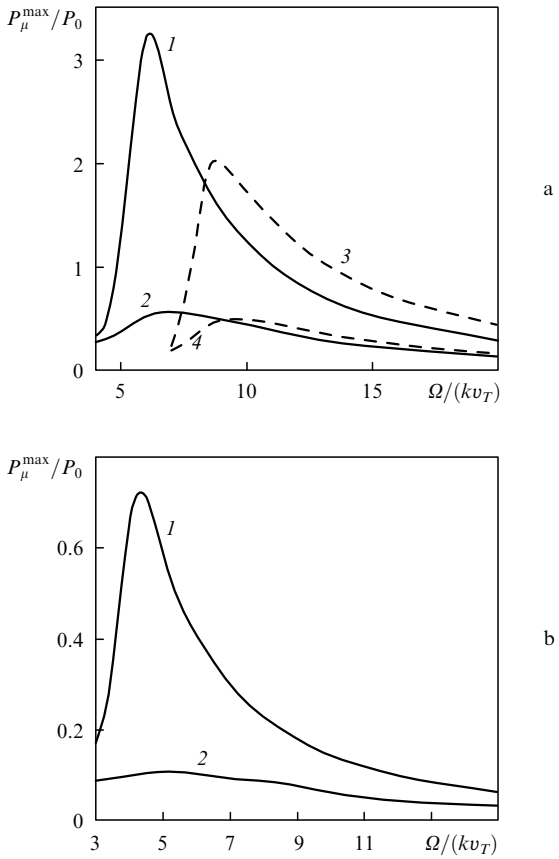

Figure 5. Dependence of the resonance amplitude in the vicinity of $\Omega_\mu \approx \Omega$ on the strong field frequency detuning in the case of phase memory conservation during collisions at transitions between the magnetic sublevels of the ground state hyperfine structure ($\tilde{v} = v = v_{tr}$), $T = 300$ K, $v_1 = v$ for ^{87}Rb (*1*, *2*) and ^{133}Cs atoms (*3*, *4*) for $I = 10^{-3}$ W cm^{-2}, $v/(kv_T) = 3 \times 10^{-4}$ (*1*, *3*), $I = 1$ W cm^{-2}, $v/(kv_T) = 9 \times 10^{-3}$ (*2*), and $I = 1$ W cm^{-2}, $v/(kv_T) = 2 \times 10^{-2}$ (*4*) (a), as well as for ^{85}Rb atoms for $I = 10^{-3}$ W cm^{-2}, $v/(kv_T) = 3 \times 10^{-4}$ (*1*) and $I = 1$ W cm^{-2}, $v/(kv_T) = 6 \times 10^{-3}$ (*2*) (b).

and achieves its maximum for a certain Ω ($\Omega \approx (6 \div 7)kv_T$ for ^{87}Rb atoms, $\Omega \approx (9 \div 10)kv_T$ for ^{133}Cs atoms, and $\Omega \approx (4 \div 5)kv_T$ for ^{85}Rb atoms). Then, the resonance amplitude decreases with increasing Ω.

Analysis shows that for a large-amplitude resonance ($P_\mu^{\max}/P_0 \sim 1$) to appear in the line wing, the absorption lines at the $m-l$ and $k-l$ transitions should be well-separated, i.e., the spacing between the excited-state hyperfine components should be larger than, or of the order of, the Doppler broadening of the line:

$$\omega_{km} \gtrsim k_\mu v_T. \tag{34}$$

For $\omega_{km} \ll k_\mu v_T$, the resonance amplitude is always small, i.e. $P_\mu^{\max}/P_0 \ll 1$. In the limiting case $\omega_{km} = 0$, the resonance is altogether absent. This circumstance is also responsible for a decrease in the resonance amplitude with increasing Ω (see Fig. 5): for large detunings Ω compared to the frequency ω_{km}, the hyperfine splitting is manifested weakly. It follows hence that among the alkali metal atoms, the most suitable objects for observing ultranarrow resonance in the absorption line wing are the ^{85}Rb, ^{87}Rb and ^{133}Cs atoms, which have a large hyperfine splitting in an excited state. For these atoms, the parameter $\omega_{km} \times (k_\mu v_T)^{-1}$ for $T = 300$ K is equal to 1.19, 2.69 and 5.39, respectively. For ^{23}Na atoms at $T = 300$ K, this parameter is quite small [$\omega_{km}/(k_\mu v_T) = 0.24$] and hence their resonance amplitude is also small [$P_\mu^{\max}/P_0 = 0.01$ for the same values of parameters as for ^{87}Rb atoms (see Fig. 2a)].

2.3 Application of a magnetic field for recording a resonance in the case of identical frequencies of the strong and probe-field waves

Expression (19) for the absorption probability of the probe field can be easily generalised to the case of atoms located in a magnetic field. For this purpose, it is sufficient to take into account the atomic level shifts in a magnetic field.

Let the atoms be located in a magnetic field $\boldsymbol{B}$ whose direction coincides with the direction of propagation of the strong and probe radiation. An atom in the $|JIFM\rangle$ state acquires the additional energy in the external magnetic field [10]

$$\Delta E = \mu_B g_F B M,$$

$$g_F = g_J \frac{F(F+1) + J(J+1) - I(I+1)}{2F(F+1)}, \tag{35}$$

$$g_J = 1 + \frac{J(J+1) - L(L+1) + S(S+1)}{2J(J+1)},$$

where μ_B is the Bohr magneton; L and S are the total orbital angular momentum and the total spin of the electrons, respectively. According to (35), we obtain the following expressions for the frequencies $\omega_{ij}(B)$ of the $i-j$ transitions in a magnetic field:

$$\omega_{mn}(B) = \omega_{mn} - \frac{\alpha_2}{6}\frac{\mu_B B}{\hbar}, \quad \omega_{ml}(B) = \omega_{ml} - \frac{7\alpha_3}{6}\frac{\mu_B B}{\hbar},$$

$$\omega_{km}(B) = \omega_{km} + \frac{\alpha_1}{3}\frac{\mu_B B}{\hbar}, \tag{36}$$

where ω_{ij} is the $i-j$ transition frequency in the absence of a magnetic field, and α_{1-3} are numerical coefficients. For alkali metal atoms with the nuclear spin $I = 3/2$ (^{7}Li, ^{23}Na, ^{39}K, ^{41}K and ^{87}Rb atoms), $\alpha_{1-3} = 1$. For ^{85}Rb atoms with $I = 5/2$, $\alpha_1 = 4/3$, $\alpha_2 = 10/3$, $\alpha_3 = 22/21$. For ^{133}Cs atoms ($I = 7/2$), $\alpha_1 = 3/2$, $\alpha_2 = 9/2$, and $\alpha_3 = 15/14$. Therefore, the resonance near $\Omega_\mu \approx \Omega$ in the presence of a magnetic field can be described by making substitutions:

$$\Omega \to \Omega(B), \quad \Omega_\mu \to \Omega_\mu(B), \quad \omega_{km} \to \omega_{km}(B) \tag{37}$$

for $\lambda_{1-3}(\boldsymbol{v})$ in (12), where

$$\Omega(B) \equiv \omega - \omega_{mn}(B) = \Omega + \frac{\alpha_2}{6}\frac{\mu_B B}{\hbar},$$

$$\Omega_\mu(B) \equiv \omega_\mu - \omega_{ml}(B) = \Omega_\mu + \frac{7\alpha_3}{6}\frac{\mu_B B}{\hbar}, \tag{38}$$

$$\Omega_\mu(B) - \Omega(B) = \omega_\mu - \omega + (7\alpha_3 - \alpha_2)\frac{\mu_B B}{6\hbar}.$$

Thus, the resonance we are interested in can be recorded by changing the magnetic field for fixed radiation frequencies. The difference in the detunings of the probe and strong fields depends linearly on the magnetic field strength. Therefore, a change in the magnetic field is equivalent to a change in the probe field frequency.

It is convenient to use the magnetic field for recording a resonance in the case of identical frequencies of the strong and probe waves (for $\omega_\mu = \omega$ or, which is the same, for $\Omega_\mu = \Omega$). It is also important that mutually correlated strong and probe waves with the same frequency can be easily obtained from one laser. In fact, it is necessary for this purpose that the radiation would have elliptic polarisation, close to circular polarisation. Indeed, such radiation can be represented as a superposition of the strong and weak light waves with mutually orthogonal circular polarisations. In this case, the weak-wave intensity will be determined by the extent of deviation of radiation polarisation from circular polarisation: the closer polarisation to circular polarisation, the lower the intensity of the probe wave.

Let us determine the magnetic field B_{res} near which a resonance appears in the probe wave radiation spectrum in the case of identical frequencies of the strong and probe waves. By using substitution (37) for $\Omega_\mu = \Omega$, we obtain from (27), within small corrections of the order of $\mu_B B/(\hbar|\Omega|) \ll 1$ and $\mu_B B/(\hbar|\Omega - \omega_{km}|) \ll 1$, the expressions

$$B_{\text{res}} = \frac{\hbar}{\mu_B}\left(\frac{|G|^2}{|\Omega|} + \frac{3|G|^2}{|\Omega - \omega_{km}|}\right) \quad (^{87}\text{Rb atoms}),$$

$$B_{\text{res}} = \frac{3\hbar}{2\mu_B}\left(\frac{|G|^2}{|\Omega|} + \frac{5|G|^2}{|\Omega - \omega_{km}|}\right) \quad (^{85}\text{Rb atoms}), \tag{39}$$

$$B_{\text{res}} = \frac{2\hbar}{\mu_B}\left(\frac{|G|^2}{|\Omega|} + \frac{7|G|^2}{|\Omega - \omega_{km}|}\right) \quad (^{133}\text{Cs atoms}).$$

The value of B_{res} is proportional to the radiation intensity and is nearly inversely proportional to the detuning Ω.

The width ΔB of the resonance (in Gauss) is described by the expressions

$$\Delta B = \frac{2\hbar\Gamma_w}{\mu_B} \quad (^{87}\text{Rb atoms}),$$

$$\Delta B = \frac{3\hbar\Gamma_w}{\mu_B} \quad (^{85}\text{Rb atoms}), \tag{40}$$

$$\Delta B = \frac{4\hbar\Gamma_w}{\mu_B} \quad (^{133}\text{Cs atoms}),$$

where Γ_w is the resonance half-width in s^{-1} [see (29)]. If the phase memory is preserved during collisions at transitions between the magnetic sublevels of the ground-state hyperfine structure or for low buffer gas pressures (when the relation $\Gamma_1 \ll \gamma$ is satisfied, so that $\Gamma_w = \gamma$), the resonance width ΔB, like the magnetic field B_{res}, is proportional to the strong-radiation intensity.

Figure 6 shows the dependence of the absorption probability of the probe radiation on the magnetic field for the ^{87}Rb atoms for exactly equal frequencies of the strong and probe radiation [calculated from (19) taking substitution (37) into account]. For parameters $I = 1$ W cm^{-2}, and $\Omega/(kv_T) = 10$, the resonance appears in the magnetic field $B_{res} = 264$ mG, and the resonance width is $\Delta B = 1.9$ mG.

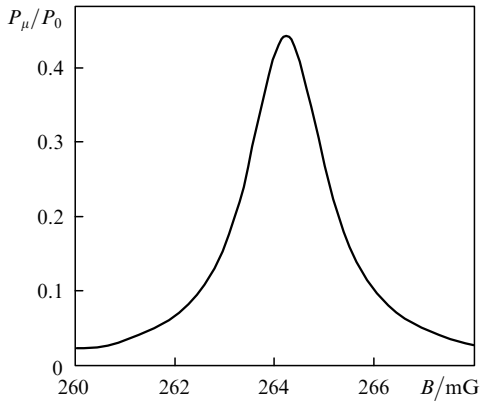

Figure 6. Dependence of the absorption probability of probe radiation on magnetic field for ^{87}Rb atoms for an exact equality of strong and probe field radiation frequencies ($\omega_\mu = \omega$ or, which is the same, $\Omega_\mu = \Omega$) in the case of phase memory conservation during collisions at transitions between the magnetic sublevels of the ground state hyperfine structure ($\bar{\nu} = \nu = \nu_{tr}$), $T = 300$ K, $I = 1$ W cm^{-2}, $\Omega/(kv_T) = 10$, $\nu_1 = \nu$, $\nu/(kv_T) = 9 \times 10^{-3}$.

2.4 Case of orthogonally intersecting waves

Under certain conditions, the resonance with a large amplitude at the wing of the absorption line may be observed for any alkali metal atoms. Consider the scheme of interaction of atoms with radiation in Fig. 7. Let us assume that a strong wave and a probe wave, which are resonant to the $^2S_{1/2} - {}^2P^o_{1/2}$ transition, intersect at a right angle ($\boldsymbol{k}_\mu \perp \boldsymbol{k}$). The strong wave has a right-hand circular polarisation, while the probe wave has a linear polarisation parallel to the propagation direction of the strong radiation ($\boldsymbol{E}_\mu || \boldsymbol{k}$). Under the action of the strong right-hand polarised field alone, all the atoms will occupy the ground-state $M = 2$ sublevel of the hyperfine component with $F_g = 2$ (this sublevel is indicated by the letter l in Fig. 7; the quantisation axis is chosen along the direction of the wave vector $\boldsymbol{k}$ of strong radiation). For the linearly polarised probe field, only the $|F_g = 2, M = 2\rangle \to |F_e = 2, M = 2\rangle$ transitions which cause a weak depopulation of the l level (the $l \to m$ transitions in Fig. 7), should be taken into account. Therefore, the probability of absorption of the probe field by the atoms can be determined by considering the interaction of radiation with a subsystem of four sublevels, l, m, n and p (these sublevels are indicated in bold in Fig. 7).

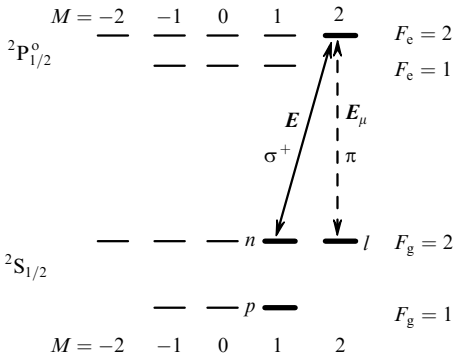

Figure 7. Energy level diagram of alkali metal atoms ^{7}Li, ^{23}Na, ^{39}K, ^{41}K, ^{87}Rb (nuclear spin $I = 3/2$) for the $^2S_{1/2} - {}^2P^o_{1/2}$ transition (D_1 line). The strong and probe waves intersect at a right angle ($\boldsymbol{k}_\mu \perp \boldsymbol{k}$). The strong wave has right-hand circular polarisation. The probe wave has linear polarisation, parallel to the direction of propagation of strong radiation ($\boldsymbol{E}_\mu || \boldsymbol{k}$). The quantisation axis is chosen along the direction of propagation of strong radiation.

The narrow resonance in the line wing near the detuning frequency of the probe field $\Omega_\mu \approx \Omega$ (or $\Omega_\mu \approx \Omega - \omega_{np}$) can be described by considering the interaction of radiation with the three-level Λ-scheme $n - m - l$ (or the Λ-scheme $p - m - l$). Thus, the expressions obtained earlier in [8] are fully applicable for calculating the probe field spectrum in this case.

A drawback of this interaction scheme is that the overlap region of orthogonally intersecting waves is small. In addition, because the modulus of the difference in the wave vectors is not small ($q \sim k$ for $\boldsymbol{k}_\mu \perp \boldsymbol{k}$), the resonance can be observed only at high buffer gas pressures so that $\nu' \gg (qv_T)$ [8]. Atomic beams can also be used for recording resonance in such an interaction scheme. In this case, the strong wave and the probe wave should be orthogonal to the atomic beam.

3. Samarium atoms

Another promising object for observing the anomalous absorption of light under nonresonance conditions is samarium atoms. Samarium has several stable isotopes with the zero nuclear spin $I = 0$: ^{152}Sm (natural abundance 26.7 %), ^{154}Sm (22.7 %), ^{148}Sm (11.3 %), ^{150}Sm (7.4 %), and ^{144}Sm (3.1 %). The analysis of anomalous absorption of light for these isotopes is simplified because they do not have a hyperfine structure of levels. We will consider below just these isotopes of Sm.

3.1 The $J_g = 1 \to J_e = 0$ transition

The $4f^6\,6s^2(^7F)$ ground energy level of Sm consists of seven fine-structure levels with the total electron moment $J_g = 0-6$ [15]. The $J_g = 1$ level has an energy of 292.58 cm^{-1}

[15]. Consider the $J_g = 1 \to J_e = 0$ transition in samarium atoms between the lowest $4f^6\,6s^2(^7F_1)$ level (with the energy 292.58 cm^{-1} and $J_g = 1$) and the excited level with the total electron angular momentum $J_e = 0$. Table 1 shows the wavelengths of some transitions. Suppose that a strong wave and a probe wave, which are resonant to the above transition, have mutually orthogonal linear polarisations. Figure 8 shows the scheme of transitions caused by the strong and probe fields (the quantisation axis z is chosen along the vector $\boldsymbol{E}$ of the strong field). In this case, two Λ-schemes, $n-m-k$ and $n-m-l$, can be distinguished.

Table 1. Wavelengths of the $J_g = 1 \to J_e = 0$ transitions in samarium atoms between the lower $4f^6\,6s^2(^7F_1)$ level (with energy 292.58 cm^{-1}) and the excited levels indicated in the table (from [15]).

Excited level	Wavelength in air/Å
$4f^6(^7F)6s\,6p(^3P^o)^7F_0^o$	4596.8
$4f^5(^6H^o)5d\,6s^2(^7F_0^o)$	5549.0
$4f^6(^7F)6s\,6p(^1P^o)^7F_0^o$	5706.8
$4f^6(^7F)6s\,6p(^3P^o)^5D_0^o$	6536.9
$4f^6(^7F)6s\,6p(^3P^o)^9G_0^o$	7403.3

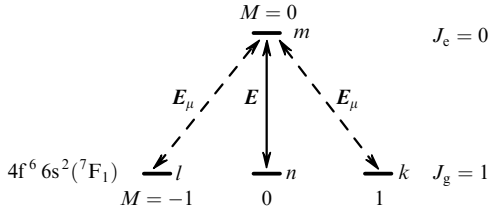

Figure 8. Energy level diagram of samarium atoms (isotopes with the zero nuclear spin) for the $J_g = 1 \to J_e = 0$ transition. The strong ($\boldsymbol{E}$) and probe ($\boldsymbol{E}_\mu$) waves have mutually orthogonal linear polarisations. The quantisation axis is chosen along the direction of the strong field vector $\boldsymbol{E}$, and the linear polarisation of the probe wave is presented as a superposition of two independent states with circular polarisations.

Let the atoms be located in a mixture with the buffer gas in a magnetic field $\boldsymbol{B}$, whose direction coincides with the strong-field vector $\boldsymbol{E}$. An atom in the state $|JM\rangle$ acquires the additional energy $\Delta E = \mu_B g_J B M$ in the external magnetic field. According to this expression, we obtain the expressions:

$$\omega_{kn}(B) = \omega_{nl}(B) = \frac{\omega_{kl}(B)}{2} = \frac{3\mu_B B}{2\hbar} \tag{41}$$

for the frequencies of $k-n$, $n-l$ and $k-l$ transitions in a magnetic field.

The polarisation of the medium at the probe field frequency is determined by the density matrix elements $\rho_{ml}(\boldsymbol{v})$ and $\rho_{mk}(\boldsymbol{v})$. They can be found from the system of kinetic equations (resonance approximation, steady-state and spatially homogeneous conditions):

$$\begin{aligned}
&\left\{\frac{\Gamma_m}{2} - \mathrm{i}[\Omega_\mu - \omega_{nl}(B) - \boldsymbol{k}_\mu\boldsymbol{v}]\right\}\rho_{ml}(\boldsymbol{v}) = S(\rho_{ml}(\boldsymbol{v})) \\
&\quad + \mathrm{i}G\rho_{nl}(\boldsymbol{v}) + \mathrm{i}G_{\mu ml}[\rho_{ll}(\boldsymbol{v}) - \rho_{mm}(\boldsymbol{v})] + \mathrm{i}G_{\mu mk}\rho_{kl}(\boldsymbol{v}), \\
&\left\{\frac{\Gamma_m}{2} - \mathrm{i}[\Omega_\mu + \omega_{kn}(B) - \boldsymbol{k}_\mu\boldsymbol{v}]\right\}\rho_{mk}(\boldsymbol{v}) = S(\rho_{mk}(\boldsymbol{v})) + \\
&\quad + \mathrm{i}G\rho_{nk}(\boldsymbol{v}) + \mathrm{i}G_{\mu mk}[\rho_{kk}(\boldsymbol{v}) - \rho_{mm}(\boldsymbol{v})] + \mathrm{i}G_{\mu ml}\rho^*_{kl}(\boldsymbol{v}),
\end{aligned} \tag{42}$$

$$\begin{aligned}
&\mathrm{i}[\boldsymbol{q}\boldsymbol{v} + \Omega - \Omega_\mu + \omega_{nl}(B)]\rho_{nl}(\boldsymbol{v}) \\
&\quad = S(\rho_{nl}(\boldsymbol{v})) + \mathrm{i}G^*\rho_{ml}(\boldsymbol{v}) - \mathrm{i}G_{\mu ml}\rho_{nm}(\boldsymbol{v}), \\
&\mathrm{i}[\boldsymbol{q}\boldsymbol{v} + \Omega - \Omega_\mu - \omega_{kn}(B)]\rho_{nk}(\boldsymbol{v}) \\
&\quad = S(\rho_{nk}(\boldsymbol{v})) + \mathrm{i}G^*\rho_{mk}(\boldsymbol{v}) - \mathrm{i}G_{\mu mk}\rho_{nm}(\boldsymbol{v}),
\end{aligned}$$

where

$$\begin{aligned}
&\Omega = \omega - \omega_{mn};\quad \Omega_\mu = \omega_\mu - \omega_{mn};\quad \boldsymbol{q} \equiv \boldsymbol{k}_\mu - \boldsymbol{k}; \\
&G = \frac{E_0}{2\hbar}\langle m|d_0|n\rangle;\quad G_{\mu mj} = \frac{E_{0\mu}}{2\hbar}\frac{\mathrm{i}}{\sqrt{2}}\langle m|d_{-1} + d_{+1}|j\rangle;\quad j = k,\, l;
\end{aligned} \tag{43}$$

Γ_m is the rate of spontaneous decay of the excited level m; ω_{mn} is the frequency of the $m-n$ transition; and $\langle i|d_\sigma|j\rangle$ are the matrix elements of the cyclic component d_σ of the dipole moment for the $|j\rangle = |J_g, M_g\rangle \to |i\rangle = |J_e, M_e\rangle$ transition. They are expressed in terms of the reduced matrix element of the dipole moment according to the Wigner–Eckart theorem [9, 10]:

$$\begin{aligned}
&\langle J_e, M_e|d_\sigma|J_g, M_g\rangle = (-1)^{J_e - M_e}\langle J_e||d||J_g\rangle \\
&\quad \times \begin{pmatrix} J_e & 1 & J_g \\ -M_e & \sigma & M_g \end{pmatrix}.
\end{aligned} \tag{44}$$

For the collision integrals in (42), we will use expressions analogous to (7) and (8):

$$\begin{aligned}
&S(\rho_{mi}(\boldsymbol{v})) = -\nu_1\rho_{mi}(\boldsymbol{v}), \\
&S(\rho_{ni}(\boldsymbol{v})) = -\nu\rho_{ni}(\boldsymbol{v}) + \tilde{\nu}\rho_{ni}W(\boldsymbol{v}),\quad i = k,\, l.
\end{aligned} \tag{45}$$

The collision integrals $S(\rho_{ni}(\boldsymbol{v}))$ take into account the possibility of preserving coherence in collisions at transitions between the magnetic sublevels of the ground-state fine structure of samarium ($\tilde{\nu} = \nu$ corresponds to complete conservation of coherence). These sublevels are weakly sensitive to atomic collisions because they are reliably screened by the outer closed shell $6s^2$ [16].

We assume below that there are no collision transitions $n \leftrightarrow k$ and $n \leftrightarrow l$ between the n, k and l levels. In this case, all the atoms will undergo transitions to the k and l levels under the action of the strong field only. Therefore, because the probe field is weak, we can assume in (42) that

$$\begin{aligned}
&\rho_{kk}(\boldsymbol{v}) = \rho_{ll}(\boldsymbol{v}) = \frac{N_1}{2}W(\boldsymbol{v}), \\
&\rho_{mm}(\boldsymbol{v}) = \rho_{kl}(\boldsymbol{v}) = \rho_{nm}(\boldsymbol{v}) = 0,
\end{aligned} \tag{46}$$

where N_1 is the equilibrium concentration of the absorbing particles at the lower $J_g = 1$ level.

Taking (45) and (46) into account, we obtain from the system of equations (42)

$$\lambda_1(\boldsymbol{v})\rho_{ml}(\boldsymbol{v}) = \mathrm{i}G_{\mu ml}\frac{N_1}{2}W(\boldsymbol{v}) + \mathrm{i}G\rho_{nl}(\boldsymbol{v}),$$

$$\lambda_2(\boldsymbol{v})\rho_{nl}(\boldsymbol{v}) = \tilde{\nu}\rho_{nl}W(\boldsymbol{v}) + \mathrm{i}G^*\rho_{ml}(\boldsymbol{v}),$$

$$\lambda_3(\boldsymbol{v})\rho_{mk}(\boldsymbol{v}) = \mathrm{i}G_{\mu mk}\frac{N_1}{2}W(\boldsymbol{v}) + \mathrm{i}G\rho_{nk}(\boldsymbol{v}), \tag{47}$$

$$\lambda_4(\boldsymbol{v})\rho_{nk}(\boldsymbol{v}) = \tilde{\nu}\rho_{nk}W(\boldsymbol{v}) + \mathrm{i}G^*\rho_{mk}(\boldsymbol{v}),$$

where

$$\lambda_1(\boldsymbol{v}) = \frac{\Gamma_m}{2} + \nu_1 - \mathrm{i}[\Omega_\mu - \omega_{nl}(B) - \boldsymbol{k}_\mu\boldsymbol{v}];$$

$$\lambda_2(\boldsymbol{v}) = \nu + \mathrm{i}[\boldsymbol{q}\boldsymbol{v} + \Omega - \Omega_\mu + \omega_{nl}(B)]; \tag{48}$$

$$\lambda_3(\boldsymbol{v}) = \lambda_1(\boldsymbol{v}) - 2\mathrm{i}\omega_{nl}(B);\quad \lambda_4(\boldsymbol{v}) = \lambda_2(\boldsymbol{v}) - 2\mathrm{i}\omega_{nl}(B).$$

The first and second pairs of equations in (47) form independent closed subsystems of equations. The first pair of equations describes the interaction of radiation with the three-level Λ-scheme $n-m-l$, the second one – with the three-level Λ-scheme $(n-m-k)$.

The probability P_μ of absorption of the probe field at the frequency ω_μ obtained from the system of equations (47) has the form

$$P_\mu \equiv -\frac{2}{N}\,\mathrm{Re}\left(\mathrm{i}G^*_{\mu ml}\rho_{ml} + \mathrm{i}G^*_{\mu mk}\rho_{mk}\right) = \frac{N_1}{N}(P_{\mu l} + P_{\mu k}), \tag{49}$$

$$P_{\mu l} = |G_\mu|^2\mathrm{Re}\left(I_2 - \frac{\tilde{\nu}|G|^2J_1^2}{1-\tilde{\nu}I_1}\right),$$

$$P_{\mu k} = |G_\mu|^2\mathrm{Re}\left(I_4 - \frac{\tilde{\nu}|G|^2J_2^2}{1-\tilde{\nu}I_3}\right),$$

where

$$|G|^2 = \frac{|\langle J_\mathrm{e}||d||J_\mathrm{g}\rangle|^2E_0^2}{12\hbar^2} = \frac{\lambda_3\Gamma_m I}{16\pi^2\hbar c};\quad |G_\mu|^2 = \frac{|\langle J_\mathrm{e}||d||J_\mathrm{g}\rangle|^2E_{0\mu}^2}{24\hbar^2}; \tag{50}$$

$$J_1 = \int\frac{W(\boldsymbol{v})\mathrm{d}\boldsymbol{v}}{\lambda_1(\boldsymbol{v})\lambda_2(\boldsymbol{v}) + |G|^2};\quad I_{1,2} = \int\frac{\lambda_{1,2}(\boldsymbol{v})W(\boldsymbol{v})\mathrm{d}\boldsymbol{v}}{\lambda_1(\boldsymbol{v})\lambda_2(\boldsymbol{v}) + |G|^2};$$

$$J_2 = \int\frac{W(\boldsymbol{v})\mathrm{d}\boldsymbol{v}}{\lambda_3(\boldsymbol{v})\lambda_4(\boldsymbol{v}) + |G|^2};\quad I_{3,4} = \int\frac{\lambda_{3,4}(\boldsymbol{v})W(\boldsymbol{v})\mathrm{d}\boldsymbol{v}}{\lambda_3(\boldsymbol{v})\lambda_4(\boldsymbol{v}) + |G|^2}. \tag{51}$$

The quantity $P_{\mu i}$ is the probability of absorption of probe radiation by three-level particles with the Λ-scheme of levels $n-m-i$ $(i=k,\,l)$. Expression (49) for $P_{\mu i}$ exactly coincides with the corresponding expression for the three-level Λ-scheme which was analysed in detail in [8].

Expression (49) for the probability P_μ of absorption of the probe field takes a simple form in the case of the Doppler broadening for a large detuning of the strong radiation frequency,

$$|\Omega| \gg k_\mu\upsilon_T \gg \Gamma \tag{52}$$

[Γ is the homogeneous half-width of the absorption line at the $J_\mathrm{g}=1\to J_\mathrm{e}=0$ transition in samarium atoms, described by expression (30)], and for a moderate pressure of the buffer gas, such that the collision frequency satisfies the condition

$$\nu' \gg q\upsilon_T,\ \frac{|G|^2}{|\Omega|}. \tag{53}$$

In this case, the probability of probe-field absorption obtained form (49) has the form (see also [8]):

$$P_\mu = \frac{N_1}{N}\frac{|G_\mu|^2}{\Gamma}\left\{\frac{2\sqrt{\pi}\Gamma}{k_\mu\upsilon_T}\exp\left[-\left(\frac{\Omega_\mu + |G|^2/\Omega}{k_\mu\upsilon_T}\right)^2\right]\right.$$

$$+\frac{(\Gamma_1+\gamma)\gamma}{(\Gamma_1+\gamma)^2 + [\Omega_\mu - \omega_{nl}(B) - \Omega - |G|^2/\Omega]^2}$$

$$\left.+\frac{(\Gamma_1+\gamma)\gamma}{(\Gamma_1+\gamma)^2 + [\Omega_\mu + \omega_{nl}(B) - \Omega - |G|^2/\Omega]^2}\right\}, \tag{54}$$

where

$$\gamma = \frac{|G|^2\Gamma}{\Omega^2};\quad \Gamma_1 = (\nu - \tilde{\nu})' + \frac{(q\upsilon_T)^2}{2\nu'}. \tag{55}$$

According to (54), the probe-field spectrum consists of a Doppler contour with the half-width $k_\mu\upsilon_T$, located near the line centre (in the vicinity of $\Omega_\mu = -|G|^2/\Omega$) and two Lorentzian contours with the same half-width $\Gamma_\mathrm{w} = \Gamma_1 + \gamma$ located at the far wing of the line [in the vicinity of $\Omega_\mu = \Omega + |G|^2/\Omega \pm \omega_{nl}(B)$]. The spacing between the Lorentzian contours is equal to $2\omega_{nl}(B) = \omega_{kl}(B)$. In the absence of a magnetic field, these contours merge and a single unsplit Lorentzian contour with doubled amplitude appears in the wing of the line. The ratio of the amplitude of the split resonance in the far wing of the line to the resonance amplitude near the line centre is

$$A = \frac{k_\mu\upsilon_T}{2\sqrt{\pi}\,\Gamma}\frac{\gamma}{\Gamma_1+\gamma} \tag{56}$$

and may be much larger than unity.

The resonance can be conveniently recorded by using the correlated strong wave and probe wave with identical frequencies (from the same laser). In this case, the resonance is recorded by varying the magnetic field. The magnetic field B_res near which the resonance appears, and the resonance width ΔB (the interval of values of B in which the resonance amplitude decreases by half) are described by the expressions

$$B_\mathrm{res} = \frac{2\hbar|G|^2}{3\mu_\mathrm{B}|\Omega|},\quad \Delta B = \frac{4\hbar\Gamma_\mathrm{w}}{3\mu_\mathrm{B}}. \tag{57}$$

Figure 9 shows the dependence of the probe radiation absorption probability on the magnetic field strength for samarium atoms with the nuclear spin $I=0$ for an exact equality of the frequencies of the strong and probe radiation. Calculations were performed for the $^7\mathrm{F}_1 \to {}^7\mathrm{F}_0^\mathrm{o}$ transition at 5706.8 Å, while the rate of spontaneous decay of the excited level Γ_m was set equal to $2.9\times10^6\ \mathrm{s}^{-1}$ [17]. According to the data obtained in [18], the degree of conservation of the phase memory $\tilde{\nu}'/\nu'$ in collisions at the transitions between the magnetic sublevels of the ground state was set equal to 0.997 (the impact broadening of the lines caused by transitions between the ground-state fine-structure levels of samarium is 300 times weaker than the impact broadening of conventional resolved lines). The values of P_μ were measured in units of P_0, which is the

probability of absorption of probe radiation tuned at the transition-line centre in the limit of a low intensity of the strong field [in the case of the Doppler broadening, the value of P_0 is determined by (25) taking the factor N_1/N into account]. For $I = 1$ W cm^{-2}, $\Omega/(kv_T) = 5$, and $v'/(kv_T) = 8 \times 10^{-5}$ (Fig. 9), the resonance in the line wing appears in the magnetic field $B_{res} = 5.9$ mG, the resonance width is $\Delta B = 0.2$ mG, and the resonance amplitude is approximately 3.5 times ($P_\mu^{max}/P_0 \simeq 3.5$) larger than the amplitude of the broad resonance (with the Doppler width) near the line centre.

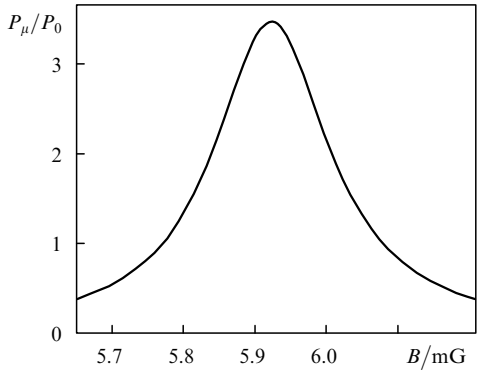

Figure 9. Dependence of the absorption probability of probe radiation on the magnetic field for samarium atoms with the zero nuclear spin in the case of copropagating waves ($\boldsymbol{q} = 0$) for the strong and probe waves with exactly equal frequencies, $T = 600$ K, $I = 1$ W cm^{-2}, $\Omega(kv_T)^{-1} = 5$, $v_1 = v$, $v'/(kv_T) = 8 \times 10^{-5}$, $\tilde{\nu}'/\nu' = 0.997$.

Figure 10 shows the dependence of the resonance amplitude on the collision frequency. At first, the resonance amplitude increases with v' and achieves its maximum for the collision frequency $v'/(kv_T) = 8 \times 10^{-5}$. This collision frequency corresponds to a buffer gas pressure of the order of 0.1 Torr. Then, the resonance amplitude decreases with increasing v'. Such a dependence of P_μ^{max} on v' is quite understandable. Indeed, according to [8], the relative amplitude P_μ^{max}/P_0 of the resonance must be equal to 1/2 in the absence of collisions (for a three-level Λ-scheme, $P_\mu^{max}/P_0 = 1$ in the absence of collisions [8], while in our case the resonance amplitude decreases by half due to splitting). As the collision frequency increases, the resonance amplitude increases due to the Dicke effect of collisional narrowing, which is manifested strongly for collision frequencies that are several orders of magnitude lower than the Doppler width [8]. Then, the resonance amplitude decreases with increasing v' in accordance with (56) (due to the presence of Γ in the denominator). A further decrease in the amplitude is caused by a partial phase memory and is manifested at $(\nu - \tilde{\nu})' > \gamma$.

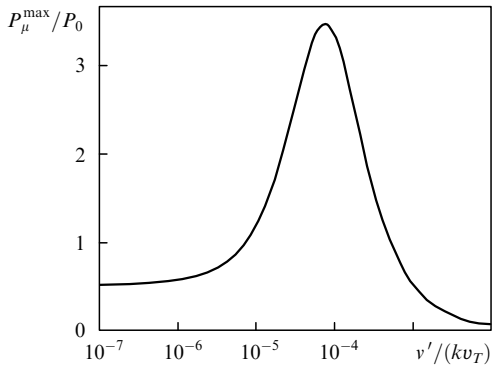

Figure 10. Dependence of the resonance amplitude in the wing of the absorption line for samarium atoms on the collision frequency. The parameters are the same as in Fig. 9.

3.2 The $J_g = 1 \rightarrow J_e = 1$ transition

An ultranarrow resonance with a large amplitude in the wing of the absorption line can also be observed in samarium atoms at the $J_g = 1 \rightarrow J_e = 1$ transition between the lower $4f^6\,6s^2(^7F_1)$ level and the excited level with the total electron angular momentum $J_e = 1$. The wavelengths of some transitions are presented in Table 2. Let us assume that a strong wave and a probe wave, which are resonant to this transition, have mutually orthogonal (right- and left-hand) circular polarisations. Figure 11 shows the scheme of transitions caused by these waves. Under the action of the strong right-hand polarised field, only one $M = 1$ sublevel at the lower $J_g = 1$ level will be populated (this sublevel is indicated by the letter l in Fig. 11). When the left-hand polarised probe field is switched on, only the $|J_g = 1, M = 1\rangle \rightarrow |J_e = 1, M = 0\rangle$ transition which weakly depopulates the l level should be taken into account. As a result, only one Λ-scheme of the $n - m - l$ levels is selected (these levels are indicated in bold in Fig. 11).

Table 2. Wavelengths of the $J_g = 1 \rightarrow J_e = 0$ transitions in samarium atoms between the lower $4f^6\,6s^2(^7F_1)$ level (with energy 292.58 cm^{-1}) and the excited levels indicated in the table (from [15]).

Excited level	Wavelength in air/Å
$4f^6(^7F)6s\,6p(^3P^o)^7F_1^o$	4539.9
$4f^5(^6H^o)5d\,6s^2(^7F_1^o)$	5498.2
$4f^6(^7F)6s\,6p(^1P^o)^7D_1^o$	6096.6
$4f^6(^7F)6s\,6p(^1P^o)^7G_1^o$	6509.5
$4f^6(^7F)6s\,6p(^3P^o)^9F_1^o$	6861.0
$4f^6(^7F)6s\,6p(^3P^o)^9G_1^o$	7293.6

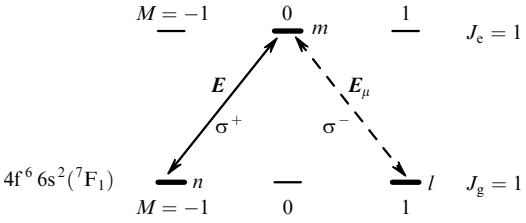

Figure 11. Energy level diagram of samarium atoms (isotopes with the zero nuclear spin) for the $J_g = 1 \rightarrow J_e = 1$ transition. The strong ($\boldsymbol{E}$) and probe ($\boldsymbol{E}_\mu$) waves which are resonant to this transition, have mutually orthogonal (right- σ^+ and left-hand σ^-) circular polarisations and propagate in the same direction. The quantisation axis is chosen along the direction of radiation propagation.

Thus, the expressions obtained earlier in [8] are fully applicable for calculating the probe field spectrum in this case.

4. Conclusions

We have studied theoretically the spectrum of absorption of a weak probe field (in the presence of a strong field) by various atoms. It has been shown that if the Λ-schemes of

levels are singled out during the interaction of strong and probe fields with the atoms, an ultranarrow resonance with a large amplitude comparable with the amplitude of the broad resonance (with the Doppler width) can appear near the line centre in the far wing of the absorption line of the probe field (anomalous absorption of light under nonresonance conditions). The ultranarrow resonance in the line wing is not related to any real transitions in the atom, and its position is determined by the frequency detuning and the intensity of the strong field.

The most promising objects for observing the anomalous absorption of light under nonresonance conditions are the rubidium atoms ^{87}Rb, cesium atoms ^{133}Cs, and even isotopes of samarium with the zero nuclear spin. For rubidium and cesium atoms, the strong and probe waves which are resonant to the $^2S_{1/2} - {}^2P^o_{1/2}$ transition should have mutually orthogonal (left- and right-hand) circular polarisations. During absorption of light at the $J_g = 1 \to J_e = 1$ transition in samarium atoms, the strong wave and the probe wave should have mutually orthogonal circular polarisations, while in the case of absorption at the $J_g = 1 \to J_e = 0$ transition, they should have mutually orthogonal linear polarisations. The waves must propagate in the same direction in all cases.

Collisions start affecting the amplitude and width of the resonance for a very low collision frequency ν'_{cr} determined from condition (31). This critical frequency of collisions depends on the strong-field intensity and its frequency detuning. For $I \sim 1$ W cm^{-2} and $|\Omega| \sim 10kv_T$, the critical frequency is $\nu'_{cr} \sim 10^{-5}kv_T$, which corresponds to a buffer gas pressure of the order of 10^{-2} Torr.

The quantity $\tilde{\nu}'/\nu'$, characterising the degree of phase memory conservation during collisions at the transitions between the magnetic sublevels of the ground state of atoms, is an important parameter. If the phase memory is not preserved ($\tilde{\nu} = 0$), collisions at $\nu' > \nu'_{cr}$ will always suppress the resonance, If, on the other hand, the phase memory is preserved quite well during collisions ($1 - \tilde{\nu}'/\nu' \ll 1$), the resonance amplitude for $\nu' > \nu'_{cr}$ increases with the collision frequency (the resonance width decreases in this case), and achieves its maximum at a certain frequency. That is why inert gases should be used as the buffer gas. In an inert buffer gas atmosphere, one can expect a high degree of phase memory conservation during collisions for rubidium, cesium and samarium atoms ($1 - \tilde{\nu}'/\nu' \lesssim 10^{-6}$ for rubidium and cesium [14], $1 - \tilde{\nu}'/\nu' \sim 3 \times 10^{-3}$ for samarium [18]).

A resonance can be recorded conveniently by using correlated strong and probe waves with the same frequency (from the same laser). In this case, the resonance can be recorded by varying the magnetic field (magnetic scanning technique). The magnetic field B_{res} near which the resonance is observed and the resonance width ΔB depend on the radiation intensity, frequency detuning, and collision frequency [see expressions (39), (40) and (57)]. Weak magnetic fields $B_{res} \sim 1 - 100$ mG are required for recording the resonance. The resonance width ΔB is two-three orders of magnitude smaller than B_{res}.

The effect considered in this work can be used in ultrahigh-resolution spectroscopy and in the problem of precise measurements of the magnetic field strength.

Acknowledgements. This work was supported by the Russian Foundation for Basic Research (Grant No. 04-02-16771), the program 'Optical Spectroscopy and Frequency Standards' of the Physics division of the Russian Academy of Sciences, and under the State Programme for Support of Leading Research Schools of Russia (Grant Nos NSh-7214.2006.2 and 2006-RI-112.0/001/046).

References

1. Rautian S.G., Smirnov G.I., Shalagin A.M. *Nelineinie rezonansy v spektrakh atomov i molekul* (Nonlinear Resonances in Atomic and Molecular Spectra) (Novosibirsk: Nauka, 1979).
2. Popov A.K. *Vvedenie v nelineinuyu spektroskopiyu* (Introduction to Nonlinear Spectroscopy) (Novosibirsk: Nauka, 1983).
3. Letokhov V.S., Chebotaev V.P. *Nelineinaya lazernaya spektroskopiya sverkhvysokogo razresheniya* (Nonlinear High-resolution Laser Spectroscopy) (Moscow: Nauka, 1990).
4. Agap'ev B.D., Gorniy M.B., Matisov B.G., Rozhdestvenskii Yu.V. *Usp. Fiz. Nauk*, **163**, 1 (1993).
5. Arimondo E., in *Progress in Optics* (Amsterdam: Elsevier, 1996) Vol. 35, p. 257.
6. Scully M.O., Zubair M.S. *Quantum Optics* (Cambridge: Cambridge University Press, 1997; Moscow: Fizmatlit, 2003).
7. Mompart J., Corbalan R. *J. Opt. B: Quantum Semiclass. Opt.*, **2**, R7 (2000).
8. Parkhomenko A.I., Shalagin A.M. *Zh. Eksp. Teor. Fiz.*, **128**, 1134 (2005).
9. Varshalovich D.A., Moskalev A.N., Khersonskii V.K. *Kvantovaya teoriya uglovogo momenta* (Quantum Theory of Angular Momentum) (Leningrad: Nauka, 1975).
10. Sobel'man I.I. *Vvedenie v teoriyu atomnykh spektrov* (Introduction to the Theory of Atomic Spectra) (Moscow: Nauka, 1977).
11. Parkhomenko A.I., Shalagin A.M. *Zh. Eksp. Teor. Fiz.*, **120**, 830 (2001).
12. Chapman S., Cowling T. *Mathematical Theory of Non-Uniform Gases* (Cambridge: Cambridge University Press, 1952).
13. Radtsig A.A., Smirnov B.M. *Parametry atomov i atomnykh ionov. Spravochnik* (Handbook of Atomic and Ionic Parameters) (Moscow: Energoatomizdat, 1986).
14. Happer W. *Phys. Rep.*, **44**, 169 (1972).
15. Martin W.C., Zalubas R., Hagan L. *Atomic Energy Levels: The Rare-Earth Elements* (Washington: Institute for Basic Standart NBS, 1978).
16. Aleksandrov E.B., Kotylev V.N., Vasilevskii K.P., Kulyasov V.N. *Opt. Spektros.*, **54**, 3 (1983).
17. Hannaford P., Lowe R.M. *J. Phys. B: At. Mol. Phys.*, **18**, 2365 (1985).
18. Vedenin V.D., Kulyasov V.N., Kurbatov A.L., Rodin N.V., Shubin M.V. *Opt. Spektros.*, **62**, 737 (1987).